Journal of Materials Chemistry C

ROYAL SOCIETY OF CHEMISTRY

PAPER

View Article Online
View Journal | View Issue

Cite this: J. Mater. Chem. C, 2023, 11, 9611

A skin-friendly soft strain sensor with direct skin adhesion enabled by using a non-toxic surfactant†

Haechan Park,‡[a] Myeonghyeon Na,‡[a] Donghyung Shin,‡[a] Daeun Kim,[a] Euna Kim,[b] Sehyun Kim,[a] Donghyun Lee[b] and Kyoseung Sim*[ac]

Received 31st March 2023,
Accepted 9th June 2023

DOI: 10.1039/d3tc01150j

rsc.li/materials-c

Wearable electronics, particularly soft strain sensors with direct skin adhesion, play a crucial role in applications such as smart healthcare systems and human–machine interfaces. However, the existing approaches for developing dry-adhesive soft electronic materials often involve potential biotoxicity and vulnerability to humid environments. In this study, we present an eco-friendly and biocompatible surfactant-based composite for soft conductive composite, soft dry-adhesive film, and skin-adherable soft strain sensors. Utilizing polyoxyethylene sorbitan monooleate, also known as Tween 80, as a non-toxic surfactant, polydimethylsiloxane (PDMS) as an elastomeric matrix, and poly(3,4-ethylenedioxythiophene) polystyrene sulfonate (PEDOT:PSS) as a conductive pathway, the composite exhibits excellent stretchability and conductivity. The soft dry-adhesive film based on Tween 80-added PDMS features exceptional softness and adhesiveness. We demonstrate a soft strain sensor based on these composites that can be directly adhered to the skin and effectively detect various human motions involving large deformations without delamination. This approach offers a promising avenue for future wearable electronics that are safe for both humans and the environment.

1. Introductions

Soft electronics, which enable direct adhesion to the skin in a dry manner, provide significant benefits for advanced wearable electronic applications, such as smart healthcare systems and human–machine interfaces (HMIs).[1–3] Specifically, a soft strain sensor with dry-adhesiveness provides a clean, environmentally friendly skin-mounting approach that is reusable, easy to reposition, and enables conformal contact with the skin.[4] These advantages make it an excellent choice for human motion monitoring, as it allows for comfortable and robust application on largely deformable body joints (*e.g.*, fingers, knees, and elbows) due to its mechanically soft nature.[5] Over the past decades, extensive efforts have been made to develop dry-adhesive properties for wearable electronics through various approaches, such as micro/nanostructure design, van der Waals force enhancement, and elasticity modulation.[6–10] However, the limited mechanical softness and potential biotoxicity restrict their effective application to wearable platforms for the human body.

Recently, significant advancements have been achieved for dry-adhesive soft electronic materials by developing elastomeric composites based on organic materials exhibiting excellent softness and electrical characteristics.[6,11,12] Particularly, the poly(3,4-ethylenedioxythiophene) polystyrene sulfonate (PEDOT:PSS), a conductive polymer, was widely used for preparing the composite with water-soluble polymers, such as polyvinyl alcohol (PVA) and waterborne-polyurethane (WPU), due to the high miscibility

[a] Department of Chemistry, Ulsan National Institute of Science and Technology (UNIST), Ulsan, 44919, Republic of Korea. E-mail: kyos@unist.ac.kr
[b] School of Energy and Chemical Engineering, Ulsan National Institute of Science and Technology (UNIST), Ulsan, 44919, Republic of Korea
[c] Center for Wave Energy Materials, Ulsan National Institute of Science and Technology (UNIST), Ulsan, 44919, Republic of Korea

† Electronic supplementary information (ESI) available. See DOI: https://doi.org/10.1039/d3tc01150j

‡ These authors contributed equally to this work.

Kyoseung Sim

Kyoseung Sim has been an assistant professor in the Department of Chemistry at the Ulsan National Institute of Science and Technology (UNIST) since Spring 2020. He earned his PhD in Materials Science and Engineering from the University of Houston in 2018, under the supervision of Cunjiang Yu. Dr Sim's current research focuses on soft electronics, specifically organic semiconductors and their system-level applications.

of those materials.[12–14] Despite the simplicity of those approaches, the water-soluble composite involves severe issues of vulnerable nature to the environment, especially moisture. Therefore, environmentally stable materials, such as polydimethylsiloxane (PDMS), polystyrene-*block*-poly(ethylene-ran-butylene)-*block*-polystyrene (SEBS), and Ecoflex, could be promising candidates for creating composites with PEDOT:PSS to develop dry-adhesive soft electronic materials. However, the hydrophobic nature of these materials leads to immiscibility issues when creating composites with hydrophilic PEDOT:PSS.

To overcome those challenges, surfactants are widely used to facilitate the blending of immiscible hydrophobic–hydrophilic mixtures by forming emulsions.[15,16] Notably, polyoxyethylene-(10)octylphenyl ether, also known as Triton X-100, has been commonly employed for preparing the mixture of PEDOT:PSS and PDMS.[17,18] The superior properties and methodological effectiveness of Triton X-100 in forming homogenous blends are well established. However, the severely negative impacts of Triton X-100 not only on the environment and microorganisms but also on human skin are still critical issues for direct skin-mountable soft electronics.[19–21] Thus, it is urgent to develop eco-friendly and non-toxic surfactant-based composites for dry-adhesive and soft electronic materials in wearable electronics that require direct contact with the human skin, in order to prevent potential toxicity from previous approaches.

In this study, we report an eco-friendly and biocompatible surfactant-based soft conductive composite, soft dry-adhesive film and direct skin-adherable soft strain sensor. As a key component, polyoxyethylene sorbitan monooleate (Tween 80), a non-ionic surfactant, is carefully chosen due to its non-toxicity. Indeed, Tween 80 is prevalent in commercially available applications for daily life, for example, cosmetics, food, pharmaceuticals, and textiles.[22,23] Thus, high biocompatibility and low toxicity on the skin make it an excellent alternative to toxic surfactants such as Triton X-100 and sodium dodecyl sulfate (SDS). PDMS was used as an elastomeric matrix because of its high thermal and chemical stability, as well as excellent mechanical properties.[24] Tween 80 effectively induces emulsification of PEDOT:PSS and PDMS, which enables the formation of three-dimensionally (3D) networked PEDOT:PSS throughout the composite with the PDMS matrix. Thus, we successfully fabricated a highly stretchable soft conductive composite with an elongation at break and conductivity of higher than 80% and 69 S cm^{-1}, approximately. By applying Tween 80 to PDMS, a soft dry-adhesive film with large stretchability (elongation at break $\geq$850%) and high adhesiveness (21.41 ± 1.76 N m^{-1}) was achieved. We further developed a large deformable strain sensor enabling direct adherence to the skin in a dry manner using bilayer configurations with soft conductive composite and dry-adhesive films. The sensor can be repeatedly stretched and released by at least 100% with a gauge factor (GF) of about 1.66. Due to the excellent adhesion to human skin and its soft nature, the sensor can detect various human motions involving large deformation, including finger, elbow, and knee bending, without delamination. The skin-adherable soft strain sensor made by biocompatible surfactants in this work provides a plausible approach to future wearable electronics in a safe manner for both humans and the environment.

2. Experimental

Materials

PEDOT:PSS (Heraeus Clevios, PH1000) and PDMS (Sylgard 184, silicone elastomer) were purchased from Ossila and Dow-Corning, respectively. Tween 80 was purchased from Duksan Chemicals. Polystyrene substrate (PS) was purchased from SPL life sciences. Polyethylene terephthalate (PET) film was purchased from Printek. All materials were used as received without further purifications.

Preparation of the soft conductive composite

The preparation of the soft conductive composite began with the concentrating PEDOT:PSS solution. This process was performed by stirring the pristine PEDOT:PSS solution at 1000 rpm and 40 °C to achieve the desired volume. The optimization of the degree of concentration will be discussed in the Results and discussion section. The concentrated PEDOT:PSS solution was then blended with PDMS [15 : 1 (w/w) base/curing agent] and Tween 80 in various ratios (w/w), using a customized overhead stirrer at room temperature. The emulsified blends were obtained after debubbling in a vacuum oven at 50 °C for 1 min. The resultant emulsions were cast onto a custom-made mold made by PET through doctor blading on the PS substrate, followed by heating at 80 °C for 2 hours in a vacuum oven. The obtained composites exhibited a thickness of approximately 200 μm.

Preparation of soft dry-adhesive films

Firstly, liquid PDMS with a 10 : 1 weight ratio of base and curing agent was prepared. Next, Tween 80 was added to the liquid PDMS in the desired ratio, ranging from 1.0 to 3.0 wt%. The mixtures were then vigorously blended using a customized overhead stirrer, followed by debubbling in a vacuum chamber. The well-blended mixtures were cast onto a custom-made PET mold using doctor blading on the PS substrate. Thereafter, the samples were heated at 60 °C for 2 hours in a convection oven, completing the fabrication of the soft dry-adhesive films. The thickness of the adhesives is approximately 400 μm.

Fabrication of a skin-adherable soft strain sensor

The strain sensors were fabricated by integrating the soft conductive composite and dry-adhesive films in a bilayer architecture. The schematic fabrication process of device fabrication is illustrated in Fig. S1 (ESI†). First, a blended mixture containing PDMS and Tween 80 (2.5 wt%) was cast onto the mold using doctor blading to form the dry-adhesive layer. After curing the sample at 60 °C for 2 hours in a convection oven, PET mold was removed, followed by the lamination of copper tapes that can be used for interfacing with external equipment. The excellent adhesion of the dry-adhesive layer ensures firmly fixed contact. The emulsion based on PDMS, Tween 80, and doubly concentrated PEDOT:PSS (50 wt%), was coated on top of

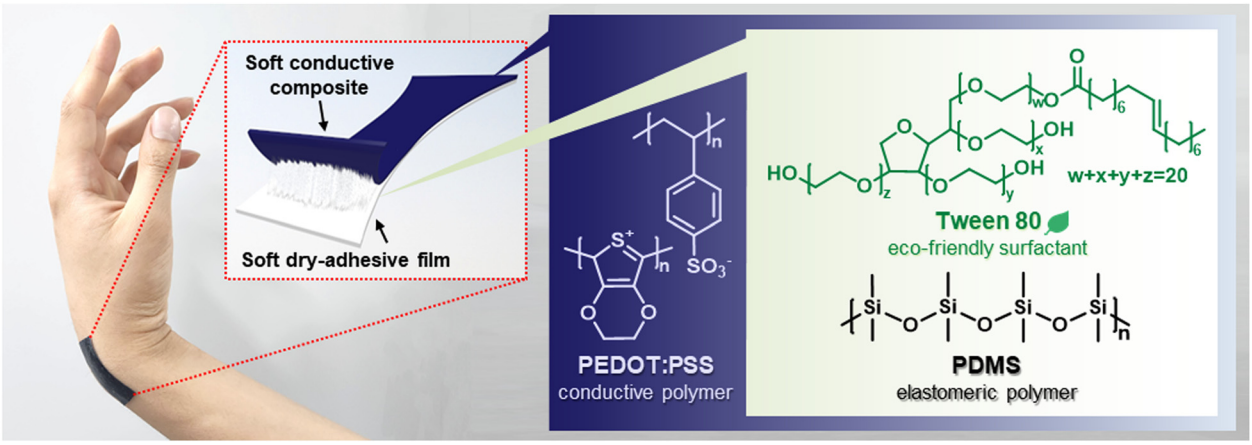

Fig. 1 Optical and schematic images of the skin-adherable soft strain sensor featuring a bilayer architecture composed of a soft conductive composite and a soft dry-adhesive film, along with the molecular structures of the individual components.

the adhesive layer using doctor blading after placing the desired shaped mold. Curing the sample at 80 °C in a vacuum oven for 2 hours allowed for the solidification of the sample. Finally, the bilayer structured strain sensor was released from the mold.

Characterization

The mechanical properties of soft conductive composite and dry-adhesive films were characterized using a motorized force tester (ESM 750, Mark-10 Corp.) equipped with force gauges (M5-2 or M5-200, Mark-10 Corp.). The force gauges were selectively used depending on the force levels. For all stretching/releasing tests, the strain rate was fixed at 50 mm min^{-1}. A constant speed of 100 cm min^{-1} was used for measuring adhesive force, which is a typical condition for peeling-based adhesion tests.[25] The semiconductor analyzer (4200-SCS, Keithley Instruments Inc.) and LCR meter (E4980A, Keysight Technology Inc.) were utilized to investigate the electrical properties of the soft conductive composite under mechanical strain using a 4-point probe, customized stretcher, and programmable stretching machine (Bending&stretchable machine system, SNM Korea). The morphologies of the soft conductive composite and dry-adhesive films were obtained using a field-emission scanning electron microscope (FE-SEM, SU7000, Hitachi Ltd.). The energy-dispersive X-ray spectroscope (EDS) equipped on the SEM was used for the elemental mapping of the soft conductive composite. The human motion monitoring capability of the skin-adherable soft strain sensor was evaluated using an LCR meter. It is noted that in all experimental characterization studies the devices are not subject to Institutional Review Board (IRB) due to their non-invasive application on skin, which do not cause physical modification to the human body, according to the Article 13, Paragraph 1 of the Enforcement Regulations of the Bioethics and Safety Act, designated by the Korean Ministry of Health and Welfare. Additionally, all figures featuring the human body were presented with the consent of the participants.

3. Results and discussion

Skin-adherable soft strain sensors

Fig. 1 illustrates a skin-adherable soft strain sensor designed for directly mounting onto the human skin, featuring a bilayer architecture with soft conductive composite and dry-adhesive films. Tween 80, a non-ionic surfactant, is eco-friendly and biocompatible, playing a crucial role in the soft conductive composites by promoting the formation of stable emulsions between the immiscible PDMS and PEDOT:PSS solution. Its high hydrophilic-to-lipophilic balance (HLB) value of 15 facilitates the formation of PDMS-in-PEDOT:PSS emulsions, with hydrophobic cores and hydrophilic shells.[26,27]

Additionally, a soft dry-adhesive film is obtained by adding Tween 80 into PDMS. This process impedes PDMS crosslinking due to the complex formation between the hydroxyl groups of Tween 80 and the Pt catalyst in the PDMS curing agent.[8,10,28] By vertically integrating the soft conductive composite with the soft dry-adhesive film, a highly stretchable ($\varepsilon > 130\%$) skin-adherable strain sensor capable of large deformation sensing is achieved. This strain sensor enables conformal mounting on the soft human skin and monitoring of various human motions, suggesting a wide range of potential advanced applications for wearable technology, particularly when directly attached to large deformable joints of the body.

Optimization of the soft conductive composite and its mechanical properties

Tween 80, with a high HLB value of 15, leads to the formation of PDMS-in-PEDOT:PSS emulsions from extremely immiscible blends. It is worth mentioning that if the PEDOT:PSS solution is used as received (pristine PEDOT:PSS), the resulting blends undergo severe phase separation, as shown in Fig. S2 (ESI†). Such phase separation results from the excessive water in the blends, thus the PEDOT:PSS solutions were concentrated before blending. Fig. S3 (ESI†) clearly demonstrates that doubly concentrated PEDOT:PSS enables the formation of a uniform composite based on blends of PDMS, PEDOT:PSS, and Tween 80.

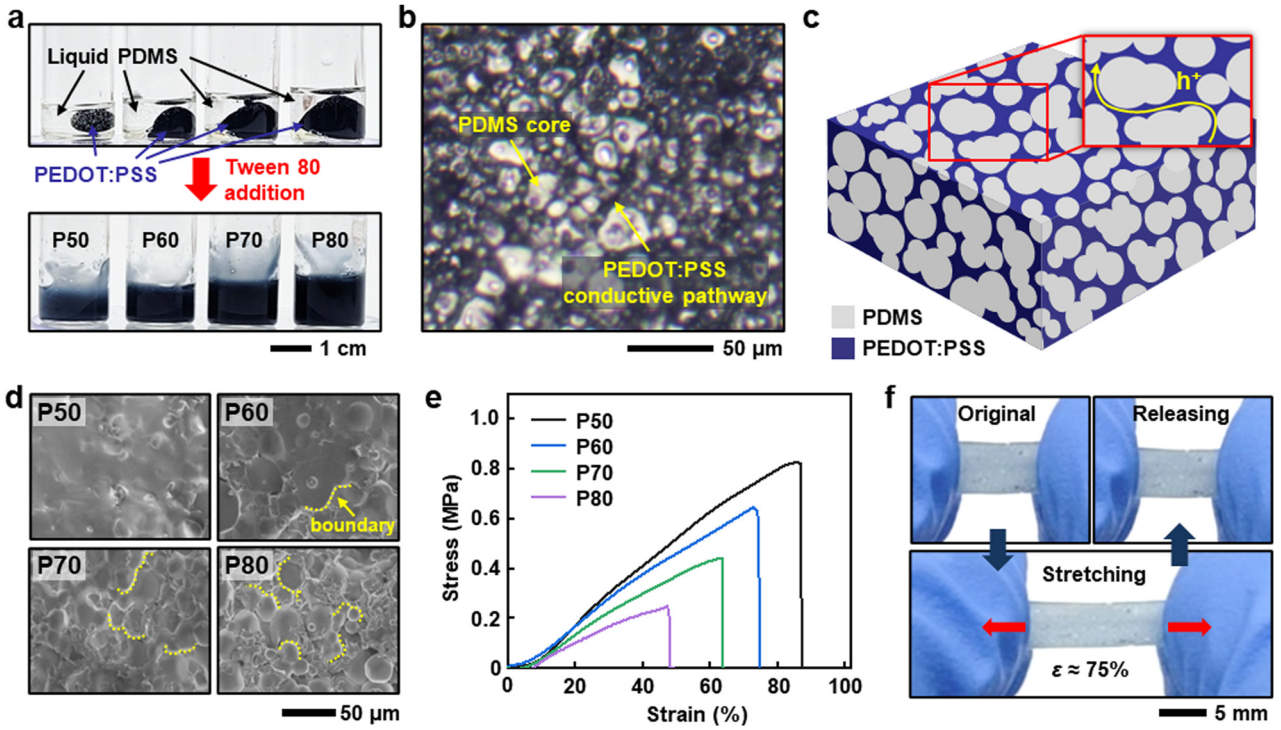

Fig. 2 Soft conductive composite and its mechanical properties. (a) Optical images of the preparation of emulsified blends with different PEDOT:PSS concentrations. (b) A cross-sectional optical microscopic image of the P50-based soft conductive composite. (c) A schematic illustration of the conduction mechanism within the soft conductive composite. (d) Cross-sectional SEM images of various soft conductive composites. (e) Stress–strain curves for the soft conductive composites. (f) Optical images of the P50-based soft conductive composite under mechanical stretching.

The concentrations of PEDOT:PSS and Tween 80 are maintained at 50 wt% and 1 wt%, respectively, relative to the PDMS weight.

Additionally, the concentration of Tween 80 relative to the PDMS weight was optimized. We investigated morphologies, mechanical, and electrical characteristics depending on the concentration of Tween 80 at 1, 3, 5, and 7 wt%. As shown in Fig. S4a (ESI†), 7 wt% Tween 80 resulted in an obvious non-uniform composite, and thus we did not investigate it further. Interestingly, a PDMS-rich layer was observed at the top side (interface between conductive area and air) of the soft conductive composite, regardless of the concentration of Tween 80, as shown in Fig. S4b and c (ESI†) This phenomenon may result from the coalescence of the released PDMS cores by thermally induced structural transition of the emulsions which shows a lower density than PEDOT:PSS[29] (0.97 g cm^{-3} for PDMS,[30] 1.0 g cm^{-3} for PEDOT:PSS[31]). Although the PDMS-rich layer is an insulator (Fig. S4d, ESI†), the composite is electrically conductive because the majority of the area consists of a uniformly distributed PEDOT:PSS, as shown in Fig. S5 (ESI†). While the electrical conductivity exhibits no obvious trends depending on the concentration of Tween 80, more Tween 80 leads to higher elongation at break due to reduced phase separation (Fig. S6, ESI†). Therefore, a Tween 80 concentration of 5 wt% relative to the amount of PDMS was chosen for further investigation and device fabrication.

The various properties of the soft conductive composites, depending on different PEDOT:PSS concentrations of 50, 60, 70, and 80 wt% relative to the PDMS weight, were investigated. It is noted that the concentration of PEDOT:PSS in the blended mixtures enabled by Tween 80 addition is denoted as P50, P60, P70, and P80, respectively (Fig. 2a). Fig. 2b shows the microstructure of the representative composite formed by P50-based emulsions. The 3D networked PEDOT:PSS through the PDMS core in the composite provides a conductive path through the composite (Fig. 2c). The microstructure of the soft conductive composite can be controlled by the amount of PEDOT:PSS relative to the PDMS. Fig. 2d shows that more PEDOT:PSS induces highly aggregated PDMS, resulting in boundary-rich morphologies. Such morphologies typically enhance the softness of materials; however, they lead to lower elongation at break due to the increased stress concentration.[32] As a result, the composite based on P50 exhibited the highest stretchability and modulus, with decreasing trends observed as the content of PEDOT:PSS increased (Fig. 2e). Fig. 2f exhibits the excellent stretchability of the P50-based composite. These results suggest that the optimized conductive composite with a sufficiently soft nature, especially a P50-based composite, is highly suitable for applications requiring significant stretchability.

Electrical properties of soft conductive composites

The electrical properties of the soft conductive composite were further characterized. Fig. 3a plots the electrical conductivity of the composite depending on PEDOT:PSS contents, showing that more PEDOT:PSS leads to higher conductivity. Among the four different conditions for the soft conductive composite, P50 and P80-based composites exhibit the lowest and highest

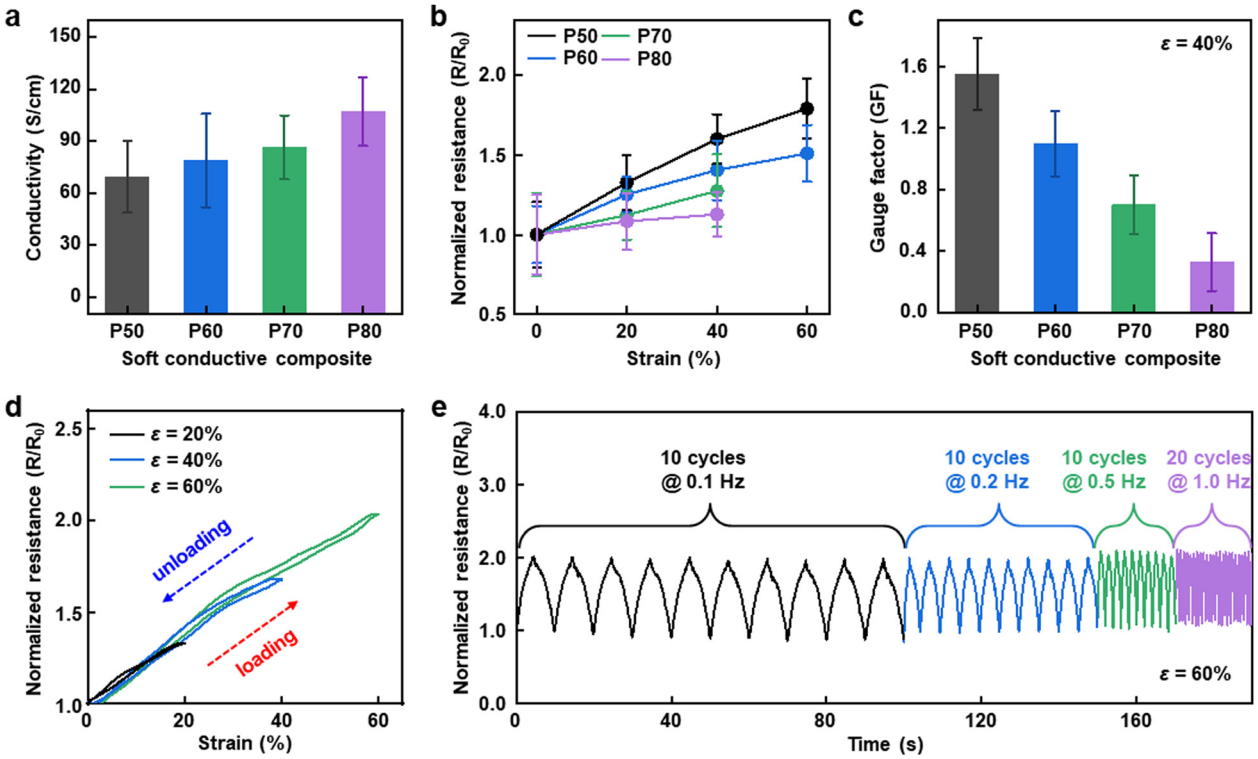

Fig. 3 Electrical properties of the soft conductive composite. (a) Electrical conductivities of the soft conductive composites (n = 8). (b) Normalized resistance changes of the soft conductive composites with different mechanical strains (n = 8). (c) Gauge factors of the soft conductive composites at 40% mechanical strain (n = 8). (d) Resistance hysteresis of the P50-based soft conductive composite within the various strains. (e) Resistance changes of the P50-based soft conductive composite depending on the repeated stretching/releasing cycles with various frequencies at 60% mechanical strain.

conductivities of 69.28 ± 20.79 and 107.03 ± 19.86 S cm^{-1}, respectively, which are comparable to the electrical properties reported in previous works.[33–35] Fig. 3b shows the normalized resistance changes of the soft conductive composite as a function of strain. On the one hand, P50 (the least soft composite) exhibits the most dramatic resistance change with the highest GF of 1.550 ± 0.232 (ε = 40%). On the other hand, P80 (the softest composite) shows the lowest GF of 0.331 ± 0.188 (ε = 40%) (Fig. 3c). These results reasonably agree with their mechanical properties, as described above. Considering mechanical stretchability and electrical conductivity, the soft conductive composite based on P50 was optimized for strain sensing; thus, we further investigate the electrical response to mechanical strain. The continuous stretching and releasing test of the P50-based composite exhibits negligible hysteresis at different strain levels (Fig. 3d). Moreover, Fig. 3e presents durable strain sensing capability under repeated stretching/releasing under a strain of 60% at different rates. These results demonstrate the potential of the soft conductive composite for use in various electronic applications, particularly as strain sensors.

Soft dry-adhesive films

Tween 80 not only allows for forming an emulsion from two immiscible materials (PDMS and PEDOT:PSS), but also enhances softness and adhesiveness when added to PDMS. Fig. 4a presents stress–strain curves of PDMS with different Tween 80 concentrations of 0, 1.0, 1.5, 2.0, and 2.5 wt%. It is worth noting that PDMS with 3.0 wt% Tween 80 showed severe residue after peeling off from an object (Fig. S7, ESI†); thus PDMS with more than 3.0 wt% Tween 80 was excluded from the further study here. From the stress–strain curves, the Young's modulus and elongation at breaks of PDMS with different Tween 80 content were extracted, as shown in Fig. 4b. These results show that as more Tween 80 was added, the PDMS became softer. Especially, the film with 2.5 wt% Tween 80 featured high stretchability and negligible hysteresis, as shown in Fig. 4c and Fig. S8 (ESI†).

The enhanced softness achieved by adding Tween 80 originates from inhibiting the crosslinking reaction between the PDMS base and the curing agent. Generally, the PDMS crosslinking involves Pt-catalyzed hydrosilylation between the vinyl-terminated prepolymer (base) and the hydrogenated curing agent.[36] In the presence of Tween 80, the polar groups in Tween 80 can form a complex with coordinatively unsaturated or free Pt in the PDMS curing agent, which induces deactivation of the Pt-catalyzed crosslinking.[10,37] Consequently, the appropriate curing inhibition results in the softening of solidified PDMS.[10] As a piece of evidence, liquid PDMS containing a sufficiently large amount of Tween 80 cannot be solidified even after 24 hours (Fig. S9, ESI†).

The soft nature of the film contributes to the enhancement of adhesion force by enabling conformal contact with surfaces, promoting van der Waals interactions.[9] Less crosslinking of PDMS results in lower packing density of molecular chains,

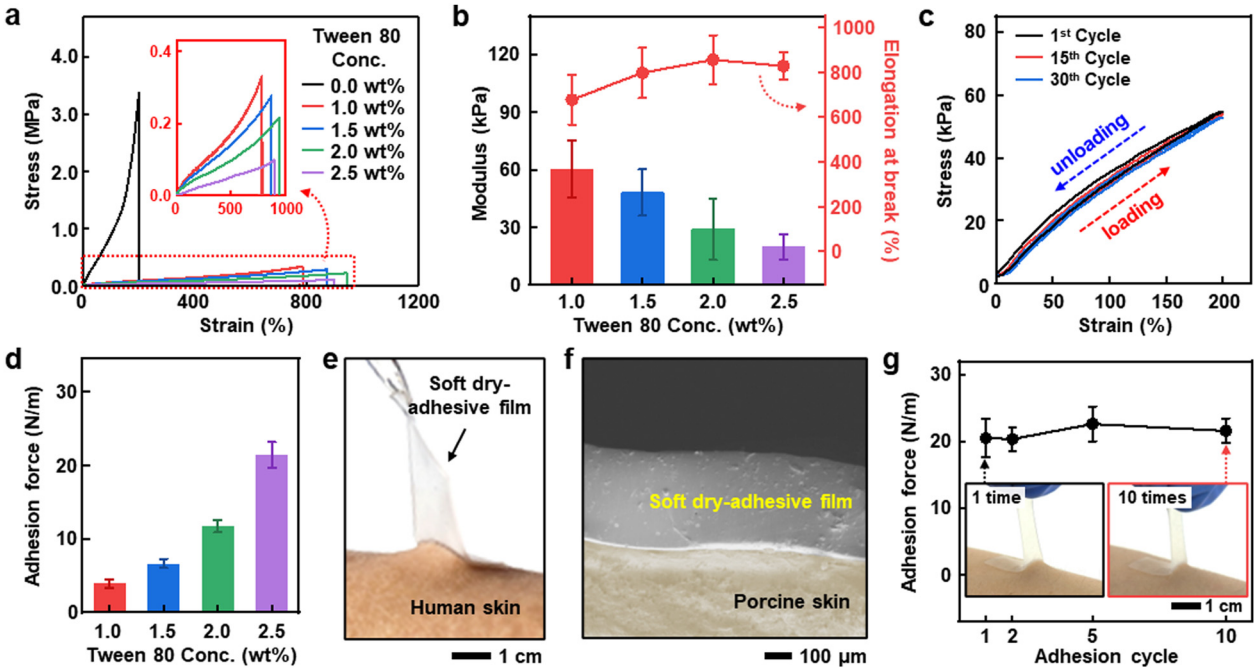

Fig. 4 Mechanical properties of the soft dry-adhesive films. (a) Stress–strain curves for the soft dry-adhesive films with different Tween 80 concentrations. (b) Modulus and elongation at break for the soft dry-adhesive films (n = 5). (c) Stress–strain hysteresis loop and cyclic stress–strain behavior of the 2.5 wt% Tween 80-added soft dry-adhesive film. (d) Adhesion forces of the soft dry-adhesive films on human skin. (e) An optical image of the 2.5 wt% Tween 80-added soft dry-adhesive film on dry human skin (n = 5). (f) Cross-sectional SEM image of the 2.5 wt% Tween 80-added soft dry-adhesive film attached to porcine skin. (g) Adhesion forces of the 2.5 wt% Tween 80-added soft dry-adhesive film during repeated adhesion cycles on dry human skin, with insets showing optical images of the film on skin during peeling off corresponding to each adhesion cycle (n = 5).

which facilitates chain diffusion inside the film, thus enhancing adhesion force.[38] Although Tween 80 leads to less crosslinking, it reacts sufficiently up to the addition of 2.5 wt%, resulting in no residue after peeling off from the surface (Fig. S10, ESI†).

The adhesive properties of PDMS with different concentrations of Tween 80 were further investigated through 180° peel-off strength test (Fig. S11, ESI†). Fig. 4d presents that the adhesion force increased as the Tween 80 concentration increased from 3.92 ± 0.56 (1.0 wt% Tween 80-added PDMS) to 21.41 ± 1.76 N m^{-1} (2.5 wt% Tween 80-added PDMS), corresponding to the abovementioned correlation between adhesiveness and the degree of crosslinking of PDMS. The 2.5 wt% Tween 80-added PDMS exhibited the highest adhesion force and softness; thus, it was selected as the soft dry-adhesive film for further studies. The film's high adhesiveness, attributed to the softening effect of Tween 80 on PDMS, allows excellent adhesion to human skin (Fig. 4e) and conformal contact with porcine skin (Fig. 4f). Owing to the dry-adhesive nature of the film, it maintains its adhesion properties with less than 4% difference after repeated attaching/detaching of at least ten times, as shown in Fig. 4g. Additionally, the film also does not leave obvious residues on the skin under repeated attaching/detaching for more than 30 times (Fig. S12, ESI†). Moreover, long-term usage on the skin for more than 24 hours does not cause skin irritation due to the biocompatible nature of both PDMS and Tween 80 (Fig. S13, ESI†). Fig. S14

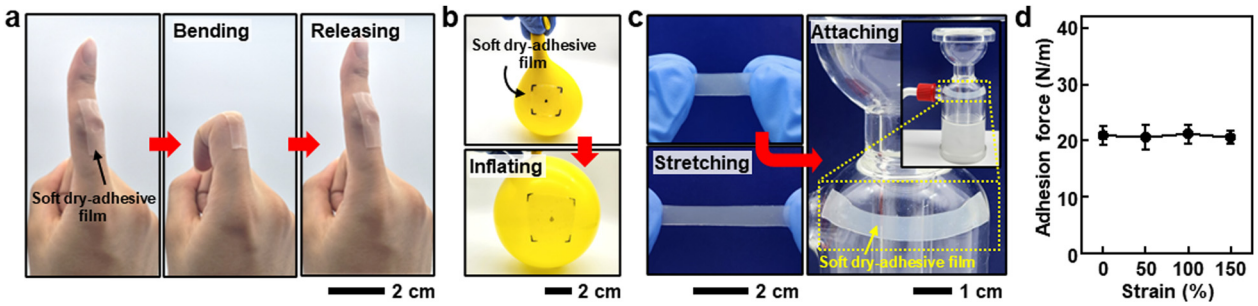

Fig. 5 Various adhesive properties of the soft dry-adhesive film. (a–c) Optical images of the 2.5 wt% Tween 80-added soft dry-adhesive film (a) stretched on a human finger, (b) inflated on a rubber balloon, and (c) stretched and then attached to a glass object. (d) Adhesion forces of the 2.5 wt% Tween 80-added soft dry-adhesive film when stretched by specific mechanical strains and attached to dry human skin (n = 5).

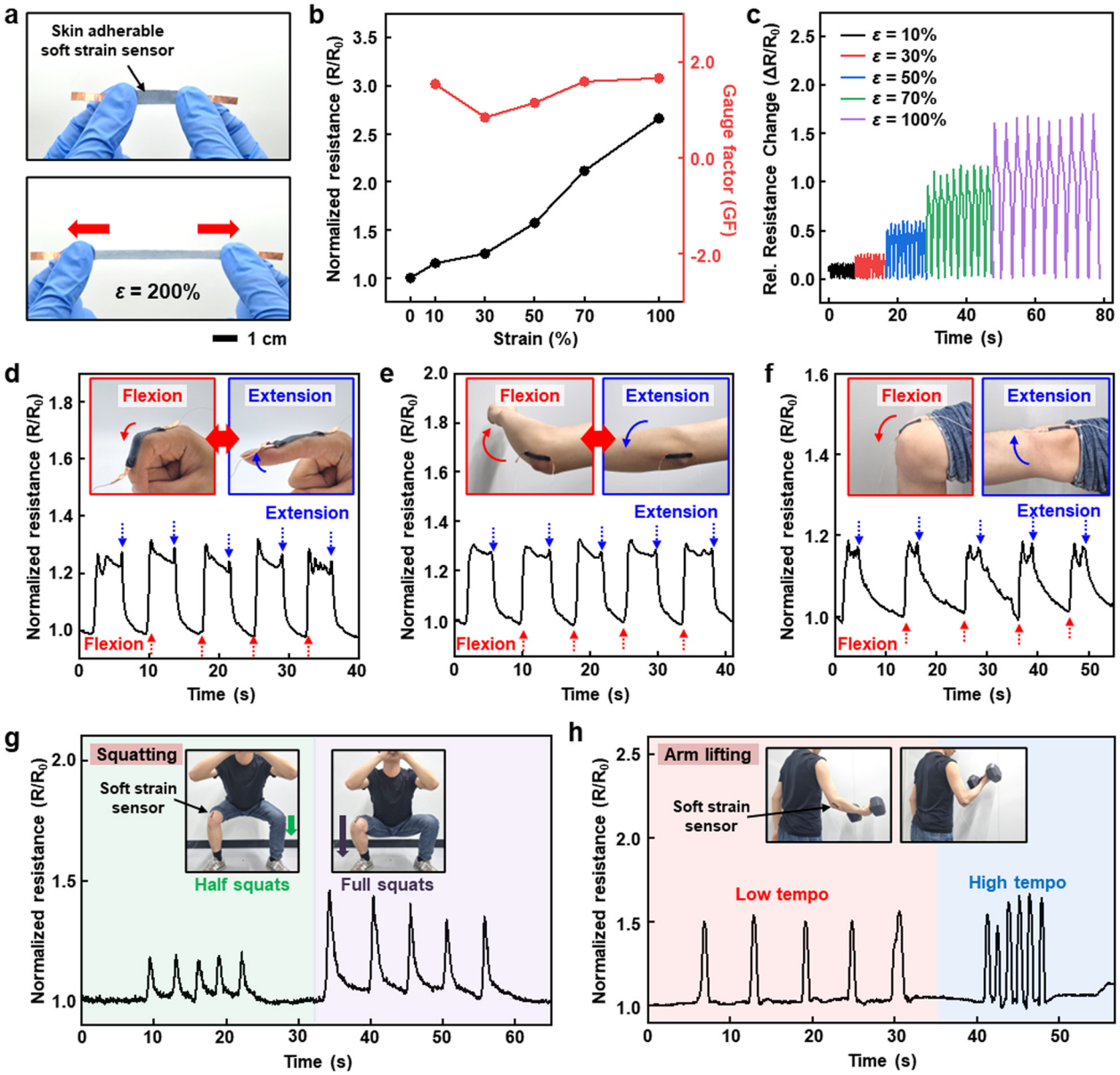

Fig. 6 Skin-adherable soft strain sensors and human motion monitoring. (a) Optical images of the skin-adherable soft strain sensors before (top) and after (down) stretching. (b) Normalized resistance changes under the various mechanical strains and corresponding gauge factors of the skin-adherable soft strain sensors. (c–h) Normalized resistance changes of the skin-adherable soft strain sensors (c) under the different repeated mechanical strains, (d) during the finger flexion/extension, (e) during the elbow flexion/extension, (f) during the knee flexion/extension, (h) during the squatting with different depths, and (g) during the arm lifting with different tempos.

(ESI†) shows the broad applicability of the soft dry-adhesive films to surfaces made of various materials.

For adhesives to be applied to direct skin-mountable soft electronics, the adhesiveness of the soft dry-adhesive film needs to be ensured under mechanical strain. Fig. 5a demonstrates that the film adheres to the proximal interphalangeal (PIP) joint during the bending of a finger, showing no delamination and, thus, no loss of adhesiveness under large mechanical strain. Additionally, the soft dry-adhesive film endures omnidirectional mechanical stretching (Fig. 5b). It is also essential for the adhesive to maintain sufficient adhesive strength to adhere to the surface of objects even after stretching. As shown in Fig. 5c, the film adheres sufficiently to a curvilinear surface after stretching by 100%. Indeed, the measured adhesion force of the soft dry-adhesive film shows no significant degradation under the mechanical strain of 150% (Fig. 5d). Additionally, the soft dry-adhesive film maintains sufficient adhesion force even while sweating after outdoor exercise, as shown in Fig. S15 (ESI†). Therefore, the soft dry-adhesive film has strong potential for a wide range of applications in direct skin-adherable electronics.

Skin-adherable soft strain sensors

We have successfully developed a strain sensor by integrating the advantageous properties of the strain-sensitive soft conductive

composite and the deformable dry-adhesive film in a bilayer architecture. Although the P50-based soft conductive composite shows an elongation at break of approximately 87% (Fig. 2e), the strain sensor exhibits excellent stretchability without fracture in the conductive composite under a strain of 200%, as shown in Fig. 6a. This enhanced stretchability of the conductive composite on the soft dry-adhesive film is attributed to the delocalization of stress concentration under mechanical deformation by the robust adhesive interface with the highly stretchable film.[39] Indeed, robust adhesion between soft conductive composite and dry-adhesive film prevents them from separating, as shown in Fig. S16 (ESI†). Due to the inhibition of crack propagation in the soft conductive composite by the well-adhered bilayer structure, the electrical property of the soft conductive composite is maintained at strains of up to approximately 130% (Fig. S17, ESI†). The characterized electrical performance of the skin-adherable soft strain sensor is shown in Fig. 6b, which presents a clear response to mechanical strain and comparable GF (1.66 at a strain of 100%) to the reported studies.[40,41] In addition, reliable resistance changes during cycling stretching/releasing at different strains were obtained (Fig. 6c).

The skin-adherable soft strain sensors on various large deformable joints of the human body were further demonstrated. The sensor shows reliable sensing capability of strain on a finger (Fig. 6d), elbow (Fig. 6e), and knee (Fig. 6f) joints without any delamination during flexion and extension. Taking advantage of the large deformable and highly adherable features, the skin-adherable soft strain sensor in this study can be utilized for regulating or monitoring exercise during fitness training. As a proof-of-concept, the strain sensors were attached to knee or elbow, which provide reliable information from typical training such as squatting depth (Fig. 6g) and lifting tempo (Fig. 6h). These results demonstrate that the skin-adherable soft strain sensor enables the detection of various human motions, offering potential for wide-ranging applications in advanced human motion monitoring.

Conclusions

In summary, we have successfully developed a skin-adherable soft strain sensor featuring a bilayer architecture with soft conductive composite and dry-adhesive films designed for directly mounting onto human skin without an additional adhesive. The eco-friendly and biocompatible Tween 80 plays a crucial role in forming the soft conductive composite, facilitating the formation of stable emulsions between PDMS and PEDOT:PSS. The soft dry-adhesive film is obtained by incorporating Tween 80 into PDMS, which softens the material and enhances its adhesiveness. We have thoroughly investigated and optimized the mechanical and electrical properties of the soft conductive composite. Moreover, we have characterized the adhesive properties of the soft dry-adhesive film under mechanical strain. The integration of the composite and film results in a strain sensor with reliable sensing capabilities that adheres well to various large deformable joints without delamination during flexion and extension. This skin-adherable soft strain sensor has potential applications in advanced human motion monitoring, including human–machine interfaces and sports performance analysis, offering a versatile tool for wearable technology.

Author contributions

H. P. and K. S. conceived and designed the experiments. H. P., M. N., D. S., D. K., E. K., S. K., and D. L. performed the experiments and obtained the data. H. P., M. N., D. S., D. K., and E. K. constructed the figures. H. P., M. N., and D. S. interpreted the data. H. P., M. N., D. S., and K. S. wrote the manuscript.

Conflicts of interest

There are no conflicts to declare.

Acknowledgements

This work was supported by the Research Funds (1.200090.01 and 1.230067.01) of Ulsan National Institute of Science & Technology (UNIST) and the National Research Foundation of Korea (NRF) grant funded by the Korean government (NRF-2021R1C1C1007714).

Notes and references

1 M. K. Choi, O. K. Park, C. Choi, S. Qiao, R. Ghaffari, J. Kim, D. J. Lee, M. Kim, W. Hyun, S. J. Kim, H. J. Hwang, S. H. Kwon, T. Hyeon, N. Lu and D. H. Kim, *Adv. Healthcare Mater.*, 2016, **5**, 80–87.
2 H. Wang, G. Pastorin and C. Lee, *Adv. Sci.*, 2016, **3**, 1500441.
3 X. Cheng, C. Bao and W. Dong, *Biomed. Microdevices*, 2019, **21**, 103.
4 H. E. Jeong and K. Y. Suh, *Nano Today*, 2009, **4**, 335–346.
5 S. Wang, Y. Fang, H. He, L. Zhang, C. A. Li and J. Ouyang, *Adv. Funct. Mater.*, 2021, **31**, 2007495.
6 S. Chun, D. W. Kim, S. Baik, H. J. Lee, J. H. Lee, S. H. Bhang and C. Pang, *Adv. Funct. Mater.*, 2018, **28**, 1805224.
7 T. Kim, J. Park, J. Sohn, D. Cho and S. Jeon, *ACS Nano*, 2016, **10**, 4770–4778.
8 S. H. Jeong, S. Zhang, K. Hjort, J. Hilborn and Z. Wu, *Adv. Mater.*, 2016, **28**, 5830–5836.
9 J. Huang, L. Cao, C. Y. Xue, Y. Z. Zhou, Y. C. Cai, H. Y. Zhao, Y. H. Xing and S. H. Yu, *Nano Lett.*, 2022, **22**, 8966–8974.
10 J. H. Kim, S. R. Kim, H. J. Kil, Y. C. Kim and J. W. Park, *Nano Lett.*, 2018, **18**, 4531–4540.
11 X. Li, Q. Shi, H. Wei, X. Zhao, Z. Tong and X. Zhu, *Biomimetics*, 2022, **7**, 167.
12 L. Zhang, K. S. Kumar, H. He, C. J. Y. Cai, X. He, H. X. Gao, S. Z. Yue, C. S. Li, R. C. S. Seet, H. L. Ren and J. Y. Ouyang, *Nat. Commun.*, 2020, **11**, 4683.
13 X. Meng, L. Mo, S. Han, J. Zhao, Y. Pan, F. Wang, Y. Fang and L. Li, *Adv. Mater. Interfaces*, 2023, **10**, 2201927.

14 J. Cao, X. Y. Yang, J. C. Rao, A. Mitriashkin, X. Fan, R. Chen, H. L. Cheng, X. C. Wang, J. Goh, H. L. Leo and J. Y. Ouyang, *ACS Appl. Mater. Interfaces*, 2022, **14**, 39159–39171.
15 J. Zhou, D. A. Khodakov, A. V. Ellis and N. H. Voelcker, *Electrophoresis*, 2012, **33**, 89–104.
16 Y. Zhang, V. Karimkhani, B. T. Makowski, G. Samaranayake and S. J. Rowan, *Macromolecules*, 2017, **50**, 6032–6042.
17 R. Luo, H. Li, B. Du, S. Zhou and Y. Zhu, *Org. Electron.*, 2020, **76**, 105451.
18 R. B. Luo, X. Li, H. B. Li, B. Du and S. S. Zhou, *Prog. Org. Coat.*, 2022, **162**, 106593.
19 J.-L. Li and B.-H. Chen, *Materials*, 2009, **2**, 76–94.
20 F. van Ruissen, M. Le, J. M. Carroll, P. G. van der Valk and J. Schalkwijk, *J. Invest. Dermatol.*, 1998, **110**, 358–363.
21 X. Ma, F. Wang and B. Wang, *J. Cosmet. Dermatol.*, 2021, **20**, 1933–1941.
22 M. A. Hamza, Z. M. Abou-Gamra, M. A. Ahmed and H. A. A. Medien, *J. Mater. Sci.: Mater. Electron.*, 2020, **31**, 4650–4661.
23 M. S. Alvarez, F. Moscoso, A. Rodriguez, M. A. Sanroman and F. J. Deive, *Bioresour. Technol.*, 2013, **146**, 689–695.
24 D. Qi, K. Zhang, G. Tian, B. Jiang and Y. Huang, *Adv. Mater.*, 2021, **33**, 2003155.
25 W. H. Yeo, Y. S. Kim, J. Lee, A. Ameen, L. Shi, M. Li, S. Wang, R. Ma, S. H. Jin, Z. Kang, Y. Huang and J. A. Rogers, *Adv. Mater.*, 2013, **25**, 2773–2778.
26 I. Ghosh and S. Mukherji, *Int. Biodeterior. Biodegrad.*, 2016, **108**, 67–75.
27 N. Anarjan and C. P. Tan, *Molecules*, 2013, **18**, 768–777.
28 C. Lou, E. Liu, T. Cheng, J. Li, H. Song, G. Fan, L. Huang, B. Dong and X. Liu, *ACS Omega*, 2022, **7**, 5825–5835.
29 S. Lehnert, H. Tarabishi and H. Leuenberger, *Colloids Surf., A*, 1994, **91**, 227–235.
30 L. H. Cai, T. E. Kodger, R. E. Guerra, A. F. Pegoraro, M. Rubinstein and D. A. Weitz, *Adv. Mater.*, 2015, **27**, 5132–5140.
31 R. Maeda, H. Kawakami, Y. Shinohara, I. Kanazawa and M. Mitsuishi, *Mater. Lett.*, 2019, **251**, 169–171.
32 R. Bai, J. Yang and Z. Suo, *Eur. J. Mech. A/Solids*, 2019, **74**, 337–370.
33 J. Y. Oh, S. Kim, H. K. Baik and U. Jeong, *Adv. Mater.*, 2016, **28**, 4455–4461.
34 P. Li, K. Sun and J. Ouyang, *ACS Appl. Mater. Interfaces*, 2015, **7**, 18415–18423.
35 P. Li, D. Du, L. Guo, Y. Guo and J. Ouyang, *J. Mater. Chem. C*, 2016, **4**, 6525–6532.
36 C. Sturgess, C. J. Tuck, I. A. Ashcroft and R. D. Wildman, *J. Mater. Chem. C*, 2017, **5**, 9733–9743.
37 C. F. Carlborg, T. Haraldsson, M. Cornaglia, G. Stemme and W. van der Wijngaart, *J. Microelectromech. Syst.*, 2010, **19**, 1050–1057.
38 X. Chu, R. Wang, H. Zhao, M. Kuang, J. Yan, B. Wang, H. Ma, M. Cui and X. Zhang, *ACS Appl. Mater. Interfaces*, 2022, **14**, 16631–16640.
39 E. J. Sawyer, A. V. Zaretski, A. D. Printz, N. V. de los Santos, A. Bautista-Gutierrez and D. J. Lipomi, *Extreme Mech. Lett.*, 2016, **8**, 78–87.
40 L. F. Wang, G. R. Gao, Y. Zhou, T. Xu, J. Chen, R. Wang, R. Zhang and J. Fu, *ACS Appl. Mater. Interfaces*, 2019, **11**, 3506–3515.
41 Z. R. He and W. Z. Yuan, *ACS Appl. Mater. Interfaces*, 2021, **13**, 1474–1485.